

The global tropospheric ammonia distribution from AIRS

J. X. Warner et al.

This discussion paper is/has been under review for the journal Atmospheric Chemistry and Physics (ACP). Please refer to the corresponding final paper in ACP if available.

The global tropospheric ammonia distribution as seen in the 13 year AIRS measurement record

J. X. Warner¹, Z. Wei¹, L. L. Strow², R. R. Dickerson¹, and J. B. Nowak³

¹Department of Atmospheric and Oceanic Science, University of Maryland College Park, College Park, MD 20742, USA

²Department of Physics and Joint Center for Environmental Technology, University of Maryland Baltimore County, Baltimore, MD 21250, USA

³Aerodyne Research, Inc., Billerica, MA 01821, USA

Received: 13 October 2015 – Accepted: 10 December 2015 – Published: 21 December 2015

Correspondence to: J. Warner (juying@atmos.umd.edu) and Z. Wei (zigangwei@gmail.com)

Published by Copernicus Publications on behalf of the European Geosciences Union.

Title Page

Abstract

Introduction

Conclusions

References

Tables

Figures



Back

Close

Full Screen / Esc

Printer-friendly Version

Interactive Discussion



The global tropospheric ammonia distribution from AIRS

J. X. Warner et al.

Title Page

Abstract

Introduction

Conclusions

References

Tables

Figures

◀

▶

◀

▶

Back

Close

Full Screen / Esc

Printer-friendly Version

Interactive Discussion



cal, scales through formation of fine ammonium containing aerosols. Ammonia reacts rapidly with sulfuric (H_2SO_4), nitric (HNO_3), and hydrochloric (HCl) acids to form a large fraction of secondary aerosols, i.e., fine Particulate Matter ($\text{PM}_{2.5}$) (particles less than $2.5\ \mu\text{m}$ in diameter) (Malm et al., 2004). These ammonium containing aerosols affect Earth's radiative balance, both directly by scattering incoming radiation and indirectly by acting as cloud condensation nuclei (e.g., Adams et al., 2001; Martin et al., 2004; Abbatt et al., 2006; Wang et al., 2008; Henze et al., 2012). A large percentage of $\text{PM}_{2.5}$ can penetrate human respiratory systems and deposit in the lungs and alveolar regions, thus endangering public health (e.g., Pope et al., 2002). Additionally, ammonia deposition increases the concentrations of the greenhouse gases nitrous oxide (N_2O) and methane (CH_4), and modifies the transport lifetimes, and deposition patterns of sulfur dioxide (SO_2) and nitrogen dioxide (NO_x). NH_3 can also contribute to increases in radiative forcing through conversion of organic carbon (OC) into brown carbon (BrC) (Updyke et al., 2012). Therefore, monitoring NH_3 global distribution of sources is vitally important to human health, with respect to air and water quality, and climate change.

Atmospheric ammonia concentrations have been modeled from a three-dimensional coupled-oxidant-aerosol model (GEOS-Chem) (Bey et al., 2001) to estimate natural and transboundary pollution influences on sulfate-nitrate-ammonium aerosol concentrations in the United States (Park et al., 2004). A number of ammonia related science studies and top-down inventory studies are based on GEOS-Chem and its ad-joint (Henze et al., 2009; Heald et al., 2012; Zhu et al., 2013; Paulot et al., 2013, 2014; Paulot and Jacob, 2014). The model's ammonia emissions were based on annual data from the $1990\ 1^\circ \times 1^\circ$ GEIA inventory of Bouwman et al. (1997). Table 1b from Park et al. (2004) shows a summary of global and contiguous US ammonia emis-sions for 2001. The inventory's categories include anthropogenic sources: domesti-cated animals, fertilizers, human bodies, industry, fossil fuels, and natural sources: oceans, crops, soils, and wild animals. Additional emissions from biomass burning and biofuel used were computed using the global inventories of Duncan et al. (2003) and Yevich and Logan (2003), with an emission factor of $1.3\ \text{g}\ \text{NH}_3\ \text{kg}^{-1}$ dry mass burned

state and the a priori state, with the weight \mathbf{A} for the true state and $\mathbf{I} - \mathbf{A}$ for the a priori. This shows the importance of AKs as diagnostics of the retrieval. The closer the matrix \mathbf{A} is to the identity matrix the more the retrieved state resembles the true state.

The optimal estimation method requires an a priori mean profile and a corresponding error covariance matrix that represent the current knowledge of the geophysical property, i.e., NH_3 , prior to the retrieval. Due to the high spatial variability and short lifetime of NH_3 , a simple fixed a priori for all emission scenarios is not appropriate. We developed a global mean, multi-year averaged (2003–2012), three-level a priori from GEOS-Chem model (v9-02) simulations for high, moderate, and low emission levels. We used GEOS-5 MERRA datasets from the NASA Global Modeling and Assimilation Office (Rienecker et al., 2011) to drive the meteorological fields in the GEOS-Chem simulations. Figure 1 shows the a priori mean profiles (solid curve with squares) and the error covariance matrices (horizontal bars) for the low emission (left panel), the moderate emission (middle panel), and the high emission levels (right panel), respectively. The high emission range was defined by profiles with Volume Mixing Ratios (VMRs) greater than or equal to 5 parts-per-billion-volume (ppbv) at surface. The moderate emission range includes the profiles with surface VMRs greater than or equal to 1 ppbv but less than 5 ppbv, or greater than 1 ppbv at any level between the surface and 500 hPa. The low emission is then defined as being lower than the lower bounds of the moderate emission range. The profiles were adjusted to match AIRS forward model levels. The modeled profiles are extrapolated near the surface with additional constraints to reflect values that are likely seen by satellite sensors.

Although for each pixel there are three possible a priori levels, the same set of the three-level a priori is used globally and throughout the AIRS data record. Thus, any spatial and temporal NH_3 variations detected using this algorithm are from AIRS measurements. To select one of the three a priori for each AIRS pixel, we examine the brightness temperature difference between a strong and a weak channel, divided by the measurement noise of the strong channel, defined as a “difference of brightness temperature index” (DBTI). This is similar to the method used by TES NH_3 and de-

The global tropospheric ammonia distribution from AIRS

J. X. Warner et al.

[Title Page](#)[Abstract](#)[Introduction](#)[Conclusions](#)[References](#)[Tables](#)[Figures](#)[◀](#)[▶](#)[◀](#)[▶](#)[Back](#)[Close](#)[Full Screen / Esc](#)[Printer-friendly Version](#)[Interactive Discussion](#)

–4 and +4 K, to avoid ambiguous a priori levels; however, this primarily affects areas over the global oceans. Any additional screening of the data for higher quality requirements, e.g. the use of DOFS, will be discussed case by case. Although we have developed AIRS NH₃ products for all available datasets, only the daytime and land cases are discussed in this study. Additionally, only radiances with quality flag as Q0 are selected for the discussions in the following sections to ensure the best accuracy.

3 Validation with in situ measurements

Validations of retrievals using in situ measurements are vital to quantifying uncertainties in the concentrations, sources, transport patterns, and trends using satellite data. Direct measurements of tropospheric NH₃ are relatively sparse and in situ measurements above the ground level, necessary to validate satellite retrievals, are available for only limited locations and time periods (e.g. Nowak et al., 2007, 2010, 2012). Validation of AIRS NH₃ datasets with available in situ measurements is a continuous effort as more in situ measurements become available. As an example of our validation effort, we use the DISCOVER-AQ NH₃ measurements over California (<https://www-air.larc.nasa.gov/cgi-bin/ArcView/discover-aq.ca-2013>). The sampling inlet and NH₃ calibration set-up used during DISCOVER AQ with the cavity ring down spectrometer (CRDS) (G2103, Picarro Inc.) is the same as used with the Chemical Ionization Mass Spectrometry (CIMS) and described in Nowak et al. (2007). The CRDS, aboard the NASA P-3B aircraft during DISCOVER-AQ CA, data period covers 16 January to 6 February 2013. We only select spiral profiles from the flights within 45 km of the center of the retrieved AIRS profiles, for the closest match, and within 3 h of the measurement window, similar to the method used for AIRS CO validation (Warner et al., 2006).

Figure 3 shows four retrieval profiles that show high NH₃ concentrations and meet the matching criteria, where the red curves represent AIRS retrieved profiles, gray curves are the a priori profiles, green solid lines are in situ spiral profiles, and the

The global tropospheric ammonia distribution from AIRS

J. X. Warner et al.

Title Page

Abstract

Introduction

Conclusions

References

Tables

Figures



Back

Close

Full Screen / Esc

Printer-friendly Version

Interactive Discussion



ber with an average value near 3.5 ppbv and decreases sharply after the SH spring season. The season of high emission in the SH is much shorter than in the NH, as demonstrated by the widths of the seasonal distribution curves. The largest SD occurs in September with a magnitude of 2 ppbv, but the variation between different years in the winter is very small (~ 0.25 ppbv).

6 Summary

AIRS ammonia (NH_3) products with a 13 year data record provide global daily maps, identify major source regions, and show seasonal cycles. This enables studies for detailed locations of the sources and their spatial and temporal variations. AIRS NH_3 products using OE retrievals provide retrieval sensitivity properties, in addition to NH_3 concentrations, such as: the AKs, error covariance matrices, and the DOFS. This will facilitate sensor inter-comparisons, model verifications, and data assimilation of satellite retrievals. AIRS measurements can not only capture high biomass burning emissions (e.g., over Russia, Alaska, South America, Africa, and Indonesia) and/or accumulated concentrations such as in various valleys (e.g., San Joaquin Valley, California in the US, the Po Valley, Italy, Fergana Valley, Uzbekistan, and the Sichuan Basin in China), but also emissions due to routine animal feeding and agriculture activities (e.g., Azerbaijan, Nile Delta and along the banks of the Nile River in Egypt, the Mid-West US, North Carolina, US, the east coast of Spain, in the Netherlands, in Mozambique and Ethiopia, Africa, and especially the Indo-Gangetic Plain of South Asia). Over China, the AIRS retrieval can match high-resolution inventories distinguishing the two major animal husbandry areas in east-central China and the Sichuan Basin. Preliminary validation results show excellent agreement with in situ airborne measurements (to within 5–15% of the retrieved profiles). Note that since each AIRS profile covers a surface area of 45 km^2 where the NH_3 amounts can vary largely, the simple numerical differences may not be the optimal way to validate satellite ammonia products.

The global tropospheric ammonia distribution from AIRS

J. X. Warner et al.

Title Page

Abstract

Introduction

Conclusions

References

Tables

Figures



Back

Close

Full Screen / Esc

Printer-friendly Version

Interactive Discussion



The global tropospheric ammonia distribution from AIRS

J. X. Warner et al.

Title Page

Abstract

Introduction

Conclusions

References

Tables

Figures



Back

Close

Full Screen / Esc

Printer-friendly Version

Interactive Discussion



We used frequent occurrences of NH_3 elevated emissions to select persistent sources. This distinguishes the NH_3 emissions due to human activities vs. occasional fires or retrieval noise. We showed the persistent ammonia sources correlate well with cropland usage, particularly in regions where irrigation is a routine practice. We showed the hemispheric seasonal variation using sources screened by the high NH_3 frequent occurrences. The NH high NH_3 emissions occur in the spring and summer with highest from April to July and lowest in November through January. In the SH, the NH_3 emission is highest in September, this is most likely due to BB emissions shown by the high VRMs and relatively low frequencies.

Detailed examinations of specific regions are needed and will be included in future studies to improve our understanding of the processes that control the NH_3 distribution and variability. The recent NH_3 trends from AIRS 13 year measurements will also be a subject of future studies since the scope of this paper is to focus on the algorithm details and the global distributions. Results in this study are focused on land and daytime only. Future studies will include more complicated surface types, i.e., ocean surfaces and regions with lower thermal contrast. The diurnal variations will also be an important topic in the future studies. We have used the pixels with the highest quality cloud-cleared radiances (at 45 km^2 spatial resolution) defined by the earlier steps of AIRS retrievals, while a future direction will be to also use the higher spatial resolution single-view pixels (at 13.5 km^2) under clear-sky conditions (Warner et al., 2013).

Acknowledgements. This study was funded by NASA's The Science of Terra and Aqua program under grant numbers NNX11AG39G and NNX12AJ05G. We wish to acknowledge the GEOS-Chem team, AIRS science team, DISCOVER-AQ team. MERRA data used in this study/project have been provided by GMAO at NASA Goddard Space Flight Center through the NASA GES DISC online archive.

References

- Abbatt, J. P. D., Benz, S., Cziczo, D. J., Kanji, Z., Lohmann, U., and Mohler, O.: Solid ammonium sulphate aerosols as ice nuclei: a pathway for cirrus cloud formation, *Science*, 313, 1770–1773, doi:10.1126/science.1129726, 2006.
- 5 Adams, P. J., Seinfeld, J. H., Koch, D., Mickley, L., and Jacob, D.: General circulation model assessment of direct radiative forcing by the sulfate–nitrate–ammonium–water inorganic aerosol system, *J. Geophys. Res.-Atmos.*, 106, 1097–1111, doi:10.1029/2000JD900512, 2001.
- 10 Adon, M., Galy-Lacaux, C., Yoboué, V., Delon, C., Lacaux, J. P., Castera, P., Gardrat, E., Pienaar, J., Al Ourabi, H., Laouali, D., Diop, B., Sigha-Nkamdjou, L., Akpo, A., Tathy, J. P., Lavenu, F., and Mougín, E.: Long term measurements of sulfur dioxide, nitrogen dioxide, ammonia, nitric acid and ozone in Africa using passive samplers, *Atmos. Chem. Phys. Discuss.*, 10, 4407–4461, doi:10.5194/acpd-10-4407-2010, 2010.
- 15 Alvarado, M. J., Cady-Pereira, K. E., Xiao, Y., Millet, D. B., and Payne, V. H.: Emission ratios for ammonia and formic acid and observations of Peroxy Acetyl Nitrate (PAN) and ethylene in biomass burning smoke as seen by the Tropospheric Emission Spectrometer (TES), *Atmosphere*, 2, 633–654, doi:10.3390/atmos2040633, 2011.
- Andreae, M. O. and Merlet, P.: Emissions of trace gases and aerosols from biomass burning, *Global Biogeochem. Cy.*, 15, 955–966, 2001.
- 20 Aneja, V. P., Chauhan, J. P., and Walker, J. T.: Characterization of atmospheric ammonia emissions from swine waste storage and treatment lagoons, *J. Geophys. Res.*, 105, 11535–11545, 2000.
- Beer, R., Shephard, M. W., Kulawik, S. S., Clough, S. A., Eldering, A., Bowman, K. W., Sander, S. P., Fisher, B. M., Payne, V. H., Luo, M., Osterman, G. B., and Worden, J. R.: First satellite observations of lower tropospheric ammonia and methanol, *Geophys. Res. Lett.*, 35, L09801, doi:10.1029/2008GL033642, 2008.
- 25 Bey, L., Jacob, D. J., Yantosca, R. M., Logan, J. A., Field, B., Fiore, A. M., Li, Q., Liu, H., Mickley, L. J., and Schultz, M.: Global modeling of tropospheric chemistry with assimilated meteorology: model description and evaluation, *J. Geophys. Res.*, 106, 23073–23096, 2001.
- 30 Bouwman, A. F., Lee, D. S., Asman, W. A. H., Dentener, F. J., VanderHoek, K. W., and Olivier, J. G. J.: A global high-resolution emission inventory for ammonia, *Global Biogeochem. Cy.*, 11, 561–587, doi:10.1029/97GB02266, 1997.

The global tropospheric ammonia distribution from AIRS

J. X. Warner et al.

Title Page

Abstract

Introduction

Conclusions

References

Tables

Figures



Back

Close

Full Screen / Esc

Printer-friendly Version

Interactive Discussion



The global tropospheric ammonia distribution from AIRS

J. X. Warner et al.

[Title Page](#)[Abstract](#)[Introduction](#)[Conclusions](#)[References](#)[Tables](#)[Figures](#)[Back](#)[Close](#)[Full Screen / Esc](#)[Printer-friendly Version](#)[Interactive Discussion](#)

Clarisse, L., Clerbaux, C., Dentener, F., Hurtmans, D., and Coheur, P.-F.: Global ammonia distribution derived from infrared satellite observations, *Nat. Geosci.*, 2, 479–483, doi:10.1038/ngeo551, 2009.

Clarisse, L., Shephard, M. W., Dentener, F., Hurtmans, D., Cady-Pereira, K., Karagulian, F., Damme, M. V., Clerbaux, C., and Coheur, P.-F.: Satellite monitoring of ammonia: a case study of the San Joaquin Valley, *J. Geophys. Res.*, 115, D13302, doi:10.1029/2009JD013291, 2010.

Coheur, P.-F., Clarisse, L., Turquety, S., Hurtmans, D., and Clerbaux, C.: IASI measurements of reactive trace species in biomass burning plumes, *Atmos. Chem. Phys.*, 9, 5655–5667, doi:10.5194/acp-9-5655-2009, 2009.

Crawford, J. H., Dickerson, R. R., and Hains, J. C.: DISCOVER-AQ: observations and early results, *Environ. Manag.*, September, 8–15, 2014.

Deeter, M. N., Edwards, D. P., Gille, J. C., and Drummond, J. R.: Sensitivity of MOPITT observations to carbon monoxide in the lower troposphere, *J. Geophys. Res.*, 112, D24306, doi:10.1029/2007JD008929, 2007.

Dentener, F. J. and Crutzen, P. J.: A three-dimensional model of the global ammonia cycle, *J. Atmos. Chem.*, 19, 331–369, 1994.

Duncan, B. N., Martin, R. V., Staudt, A. C., Yevich, R., and Logan, J. A.: Interannual and seasonal variability of biomass burning emissions constrained by satellite observations, *J. Geophys. Res.*, 108, 4100, doi:10.1029/2002JD002378, 2003.

Erismann, J. W., Galloway, J. N., Seitzinger, S., Bleeker, A., Dise, N. B., Petrescu, R., Leach, A. M., and de Vries, W.: Consequences of human modification of the global nitrogen cycle, *Philos. T. R. Soc. B*, 368, 20130116, doi:10.1098/rstb.2013.0116, 2013.

Fowler, D., Coyle, M., Skiba, U., Sutton, M. A., Cape, J. N., Reis, S., Sheppard, L. J., Jenkins, A., Grizzetti, B., Galloway, J. N., Vitousek, P., Leach, A., Bouwman, A. F., Bahl, K. B., Dentener, F., Stevenson, D., Amann, M., and Voss, M.: The global nitrogen cycle in the twenty-first century, *Philos. T. R. Soc. B*, 368, 2013016, doi:10.1098/rstb.2013.0164, 2013.

Galloway, J. N., Townsend, A. R., Erismann, J. W., Bekunda, M., Cai, Z., Freney, J. R., Martinelli, L. A., Seitzinger, S. P., and Sutton, M. A.: Transformation of the nitrogen cycle: recent trends, questions, and potential solutions, *Science*, 320, 5878, 889–892, 2008.

Haywood, J. M., Pelon, J., Formenti, P., Bharmal, N. A., Brooks, M. E., Capes, G., Chazette, P., Chou, C., Christopher, S. A., and Coe, H.: Overview of the dust and biomass-burning experi-

The global tropospheric ammonia distribution from AIRS

J. X. Warner et al.

Title Page

Abstract

Introduction

Conclusions

References

Tables

Figures



Back

Close

Full Screen / Esc

Printer-friendly Version

Interactive Discussion



ment and african monsoon multidisciplinary analysis special observing period-0, *J. Geophys. Res.*, 113, D00C17, doi:10.1029/2008JD010077, 2008.

Heald, C. L., Collett Jr., J. L., Lee, T., Benedict, K. B., Schwandner, F. M., Li, Y., Clarisse, L., Hurtmans, D. R., Van Damme, M., Clerbaux, C., Coheur, P.-F., Philip, S., Martin, R. V., and Pye, H. O. T.: Atmospheric ammonia and particulate inorganic nitrogen over the United States, *Atmos. Chem. Phys.*, 12, 10295–10312, doi:10.5194/acp-12-10295-2012, 2012.

Henze, D. K., Hakami, A., and Seinfeld, J. H.: Development of the adjoint of GEOS-Chem, *Atmos. Chem. Phys.*, 7, 2413–2433, doi:10.5194/acp-7-2413-2007, 2007.

Henze, D. K., Shindell, D. T., Akhtar, F., Spurr, R. J. D., Pinder, R. W., Loughlin, D., Kopacz, M., Sing, K., and Shim, C.: Spatially refined aerosol direct radiative forcing efficiencies, *Environ. Sci. Technol.*, 46, 9511–9518, doi:10.1021/es301993s, 2012.

Huang, X., Song, Y., Li, M., Li, J., Huo, Q., Cai, X., Zhu, T., Hu, M., and Zhang, H.: A high-resolution ammonia emission inventory in China, *Global Biogeochem. Cy.*, 26, GB1030, doi:10.1029/2011GB004161, 2012.

Kulshrestha, U. C., Granat, L., Engardt, M., and Rodhe, H.: Review of precipitation monitoring studies in India – a search for regional patterns, *Atmos. Environ.*, 39, 4419–4435, 2005.

Lin, N. H., Tsay, S. C., Maring, H. B., Yen, M.-C., Sheu, G.-C., Wang, S.-H., Chi, K. H., Chuang, M.-T., Ou-Yang, C.-F., Fu, J. S., Reid, J. S., Lee, C.-T., Wang, L.-C., Wang, J.-L., Hsu, C. N., Sayer, A. M., Holben, B. N., Chu, Y.-C., Nguyen, X. C., Sopajaree, K., Chen, S.-J., Cheng, M.-T., Tsuang, B.-J., Tsai, C.-J., Peng, C.-M., Schnell, R. C., Conway, T., Chang, C.-T., Lin, K.-S., Tsai, Y. I., Lee, W.-J., Chang, S.-C., Liu, J.-J., Chiang, W.-L., Huang, S.-J., Lin, T.-H., Liu, G.-R.: An overview of regional experiments on biomass burning aerosols and related pollutants in Southeast Asia: from BASE-ASIA and the Dongsha Experiment to 7-SEAS, *Atmos. Environ.*, 78, 1–19, doi:10.1016/j.atmosenv.2013.04.066, 2013.

Luo, M., Shephard, M. W., Cady-Pereira, K. E., Henze, D. K., Zhu, L., Bash, J. O., Pinder, R. W., Capps, S. L., Walker, J. T., Jones, M. R.: Satellite observations of tropospheric ammonia and carbon monoxide: global distributions, regional correlations and comparisons to model simulations, *Atmos. Environ.*, 106, 262–277, doi:10.1016/j.atmosenv.2015.02.007, 2015.

Malm, W. C., Schichtel, B. A., Pitchford, M. L., Ashbaugh, L. L., and Eldred, R. A.: Spatial and monthly trends in speciated fine particle concentration in the United States, *J. Geophys. Res.*, 109, D03306, doi:10.1029/2003JD003739, 2004.

Martin, S. T., Hung, H.-M., Park, R. J., Jacob, D. J., Spurr, R. J. D., Chance, K. V., and Chin, M.: Effects of the physical state of tropospheric ammonium-sulfate-nitrate particles on global

The global tropospheric ammonia distribution from AIRS

J. X. Warner et al.

Title Page

Abstract

Introduction

Conclusions

References

Tables

Figures



Back

Close

Full Screen / Esc

Printer-friendly Version

Interactive Discussion



Pinder, R. W., Walker, J. T., Bash, J. O., Cady-Pereira, K. E., Henze, D. K., Luo, M., Osterman, G. B., and Shephard, M. W.: Quantifying spatial and seasonal variability in atmospheric ammonia with in situ and space-based observations, *Geophys. Res. Lett.*, 38, L04802, doi:10.1029/2010GL046146, 2011.

5 Pope, C. A., Burnett, R. T., Thun, M. J., Calle, E. E., Krewski, D., Ito, K., and Thurston, G. D.: Lung cancer, cardiopulmonary mortality, and long-term exposure to fine particulate air pollution, *J. Am. Med. Assoc.*, 287, 1132–1141, 2002.

R'Honi, Y., Clarisse, L., Clerbaux, C., Hurtmans, D., Duflot, V., Turquety, S., Ngadi, Y., and Coheur, P.-F.: Exceptional emissions of NH₃ and HCOOH in the 2010 Russian wildfires, *Atmos. Chem. Phys.*, 13, 4171–4181, doi:10.5194/acp-13-4171-2013, 2013.

10 Rienecker, M. M., Suarez, M. J., Gelaro, R., Todling, R., Bacmeister, J., Liu, E., Bosilovich, M. G., Schubert, S. D., Takacs, L., Kim, G.-K., Bloom, S., Chen, J., Collins, D., Conaty, A., da Silva, A., Gu, W., Joiner, J., Koster, R. D., Lucchesi, R., Molod, A., Owens, T., Pawson, S., Pegion, P., Redder, C. R., Reichle, R., Robertson, F. R., Ruddick, A. G., Sienkiewicz, M., and Woollen, J.: MERRA: NASA's modern-era retrospective analysis for research and applications, *J. Climate*, 24, 3624–3648, doi:10.1175/JCLI-D-11-00015.1, 2011.

15 Rodgers, C. D.: *Inverse Methods for Atmospheric Sounding, Theory and Practice*, World Sci., River Edge, NJ, 2000.

Rodgers, C. D. and Connor, B. J.: Intercomparison of remote sounding instruments, *J. Geophys. Res.*, 108, 4116, doi:10.1029/2002JD002299, 2003.

20 Roelle, V. P. and Aneja, P. A.: *Environmental Simulation Chambers: Application to Atmospheric Chemical Processes*, Springer, 457 pp., 2002.

Shephard, M. W., Cady-Pereira, K. E., Luo, M., Henze, D. K., Pinder, R. W., Walker, J. T., Rinsland, C. P., Bash, J. O., Zhu, L., Payne, V. H., and Clarisse, L.: TES ammonia retrieval strategy and global observations of the spatial and seasonal variability of ammonia, *Atmos. Chem. Phys.*, 11, 10743–10763, doi:10.5194/acp-11-10743-2011, 2011.

25 Sommer, S. G., Schjörriing, J. K., and Denmead, O. T.: Ammonia emission from mineral fertilizers and fertilized crops, *Adv. Agron.*, 82, 557–622, 2004.

Strow, L., Hannon, S., Machado, S., Motteler, H., and Tobin, D.: An overview of the AIRS radiative transfer model, *IEEE T Geosci. Remote*, 41, 303–313, 2003.

30 Susskind, J., Barnett, C. D., and Blaisdell, J. M.: Retrieval of atmospheric and surface parameters from AIRS/AMSU/HSB data in the presence of clouds, *IEEE T. Geosci. Remote*, 41, 390–409, 2003.

The global tropospheric ammonia distribution from AIRS

J. X. Warner et al.

Title Page

Abstract

Introduction

Conclusions

References

Tables

Figures



Back

Close

Full Screen / Esc

Printer-friendly Version

Interactive Discussion

Sutton, M., Erisman, J., Dentener, F., and Moller, D.: Ammonia in the environment: From ancient times to the present, *Environ. Pollut.*, 156, 583–604, doi:10.1016/j.envpol.2008.03.013, 2008.

Sutton, M. A., Nemitz, E., Erisman, J. W., Beier, C., Bahl, K. B., Cellier, P., de Vries, W., Cotrufo, F., Skiba, U., Di Marco, C., Jones, S., Laville, P., Soussana, J. F., Loubet, B., Twigg, M., Famulari, D., Whitehead, J., Gallagher, M. W., Neftel, A., Flechard, C. R., Herrmann, B., Calanca, P. L., Schjöring, J. K., Daemmgen, U., Horvath, L., Tang, Y. S., Emmett, B. A., Tietema, A., Penuelas, J., Kesik, M., Brueggemann, N., Pilegaard, K., Vesala, T., Campbell, C. L., Olesen, J. E., Dragosits, U., Theobald, M. R., Levy, P., Mobbs, D. C., Milne, R., Viovy, N., Vuichard, N., Smith, J. U., Smith, P., Bergamaschi, P., Fowler, D., and Reis, S.: Challenges in quantifying biosphere–atmosphere exchange of nitrogen species, *Environ. Pollut.*, 150, 125–139, doi:10.1016/j.envpol.2007.04.014, 2007.

Updyke, K. M., Nguyen, T. B., and Nizkorodov, S. A.: Formation of brown carbon via reactions of ammonia with secondary organic aerosols from biogenic and anthropogenic precursors, *Atmos. Environ.*, 63, 22–31, 2012.

Walker, J. M., Philip, S., Martin, R. V., and Seinfeld, J. H.: Simulation of nitrate, sulfate, and ammonium aerosols over the United States, *Atmos. Chem. Phys.*, 12, 11213–11227, doi:10.5194/acp-12-11213-2012, 2012.

Wang, J., Jacob, D. J., and Martin, S. T.: Sensitivity of sulfate direct climate forcing to the hysteresis of particle phase transitions, *J. Geophys. Res.*, 113, D11207, doi:10.1029/2007JD009368, 2008.

Warner, J., Carminati, F., Wei, Z., Lahoz, W., and Attié, J.-L.: Tropospheric carbon monoxide variability from AIRS and IASI under clear and cloudy conditions, *Atmos. Chem. Phys. Discuss.*, 13, 16337–16366, doi:10.5194/acpd-13-16337-2013, 2013.

Warner, J. X., Comer, M. M., Barnet, C. D., McMillan, W. W., Wolf, W., Maddy, E., and Sachse, G.: A comparison of satellite tropospheric carbon monoxide measurements from AIRS and MOPITT during INTEX-A, *J. Geophys. Res.*, 112, D15, doi:10.1029/2006JD007925, 2006.

Warner, J. X., Wei, Z., Strow, L. L., Barnet, C. D., Sparling, L. C., Diskin, G., and Sachse, G.: Improved agreement of AIRS tropospheric carbon monoxide products with other EOS sensors using optimal estimation retrievals, *Atmos. Chem. Phys.*, 10, 9521–9533, doi:10.5194/acp-10-9521-2010, 2010.

**The global
tropospheric
ammonia distribution
from AIRS**

J. X. Warner et al.

[Title Page](#)[Abstract](#)[Introduction](#)[Conclusions](#)[References](#)[Tables](#)[Figures](#)[◀](#)[▶](#)[◀](#)[▶](#)[Back](#)[Close](#)[Full Screen / Esc](#)[Printer-friendly Version](#)[Interactive Discussion](#)

- Wu, S.-Y., Krishnanb, S., Zhang, Y., and Aneja, V.: Modeling atmospheric transport and fate of ammonia in North Carolina – Part I: Evaluation of meteorological and chemical predictions, *Atmos. Environ.*, 42, 3419–3436, 2007.
- 5 Yamaji, K., Ohara, T., and Akimoto, H.: Regional-specific emission inventory for NH₃, N₂O, and CH₄ via animal farming in south, southeast, and East Asia, *Atmos. Environ.*, 38, 7111–7121, 2004.
- Yevich, R. and Logan, J. A.: An assessment of biofuel use and burning of agricultural waste in the developing world, *Global Biogeochem. Cy.*, 17, 1095, doi:10.1029/2002GB001952, 2003.
- 10 Zhu, L., Henze, D. K., Cady-Pereira, K. E., Shephard, M. W., Luo, M., Pinder, R. W., Bash, J. O., and Jeong, G.-R.: Constraining US ammonia emissions using TES remote sensing observations and the GEOS-Chem adjoint model, *J. Geophys. Res.-Atmos.*, 118, 3355–3368, doi:10.1002/jgrd.50166, 2013.

The global tropospheric ammonia distribution from AIRS

J. X. Warner et al.

Title Page

Abstract

Introduction

Conclusions

References

Tables

Figures



Back

Close

Full Screen / Esc

Printer-friendly Version

Interactive Discussion

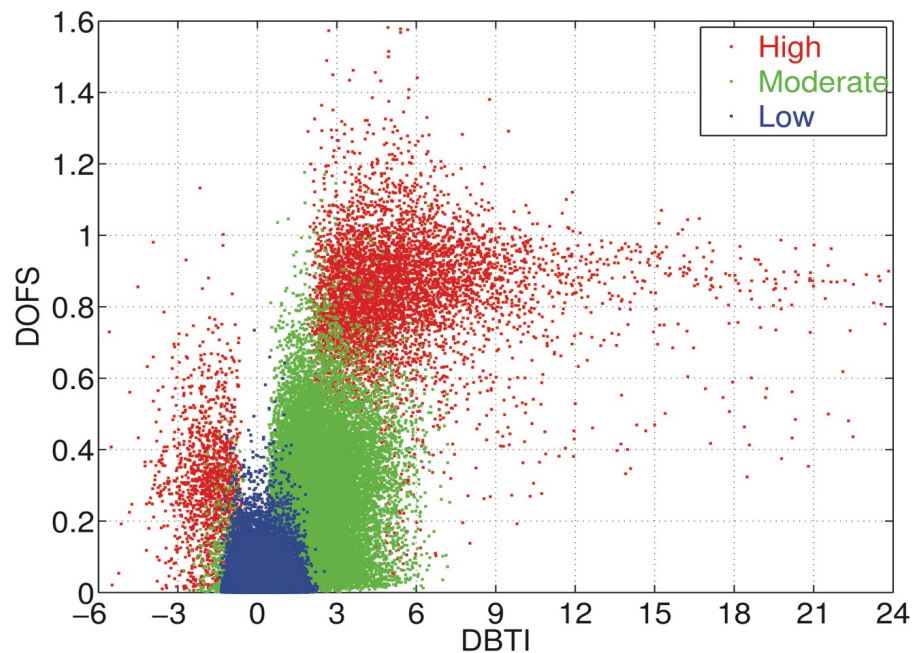


Figure 2. Correlation between the DBTI (Difference of Brightness Temperature Index) and DOFS (Degrees Of Freedom for Signal) for the three emission levels with low emissions in blue, moderate emissions in green, and high emissions in red.

The global tropospheric ammonia distribution from AIRS

J. X. Warner et al.

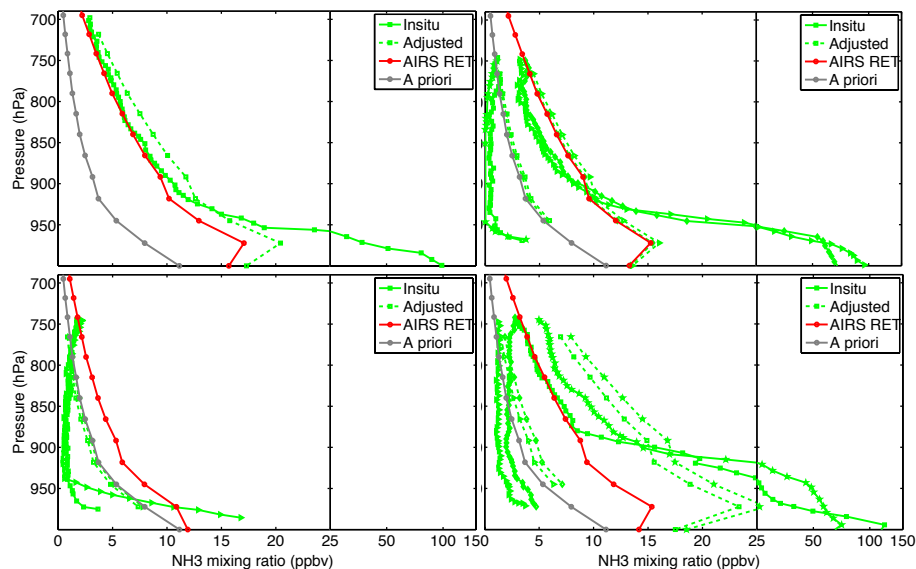


Figure 3. AIRS NH_3 validation against CRDS (the cavity ring down spectrometer) spiral profiles collected during the DISCOVER-AQ CA (16 January–6 February 2013). The red curves represent AIRS retrieved profiles, gray curves are the a priori profiles, green solid lines are in situ spiral profiles, and the green dashed lines are the convolved profiles using AIRS NH_3 AKs. The x axis is linear from 0 to 25 ppbv and logarithmic from 25 to 150 ppbv.

Title Page

Abstract

Introduction

Conclusions

References

Tables

Figures

◀

▶

◀

▶

Back

Close

Full Screen / Esc

Printer-friendly Version

Interactive Discussion



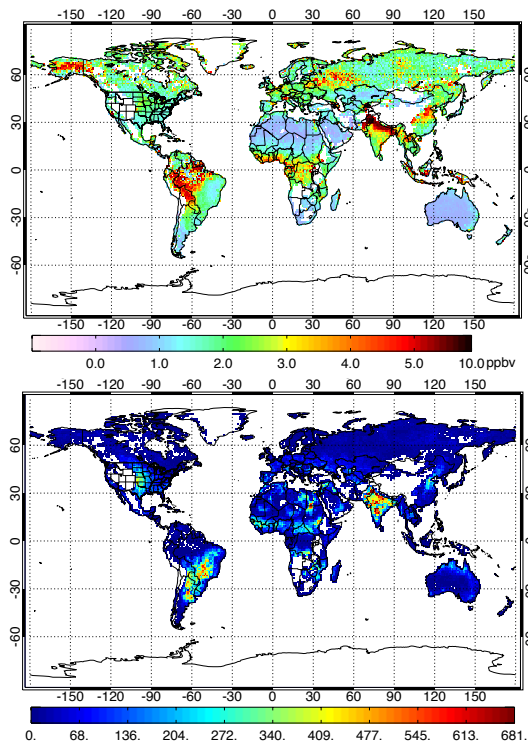


Figure 4. Upper panel: AIRS global NH₃ VMRs at 918 hPa, averaged from September 2002 through August 2015. The x axis is linear from 0 to 5 ppbv and 5 to 10 ppbv, but with different increments. Lower panel: the total occurrences (number of days) of high emissions (VMRs > 1.0 ppbv at 918 hPa) in the 13 year period. Red/blue indicate relatively high/low occurrences of high emissions, respectively.

The global tropospheric ammonia distribution from AIRS

J. X. Warner et al.

Title Page

Abstract Introduction

Conclusions References

Tables Figures

◀ ▶

◀ ▶

Back Close

Full Screen / Esc

Printer-friendly Version

Interactive Discussion



The global tropospheric ammonia distribution from AIRS

J. X. Warner et al.

Title Page

Abstract

Introduction

Conclusions

References

Tables

Figures



Back

Close

Full Screen / Esc

Printer-friendly Version

Interactive Discussion

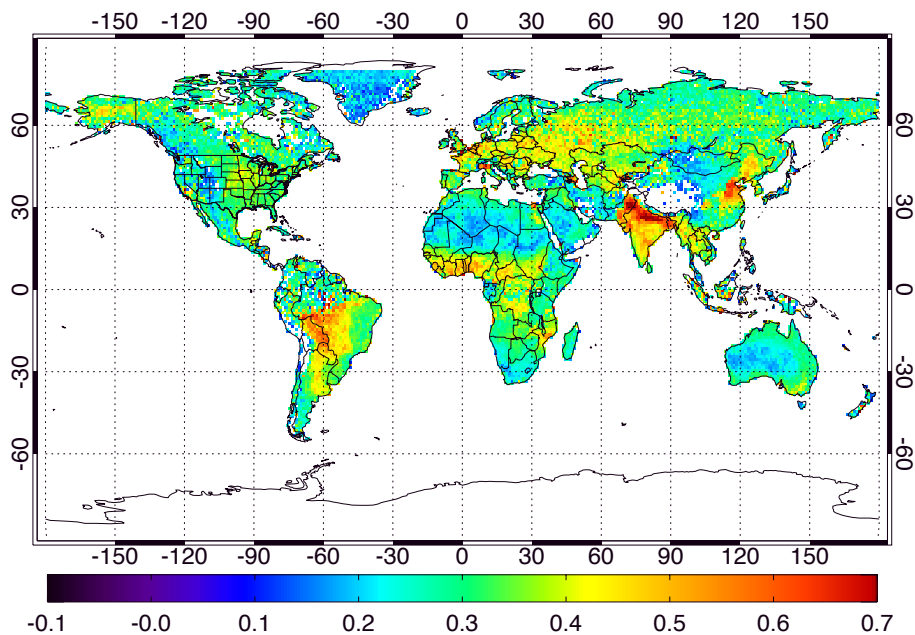


Figure 5. AIRS NH_3 DOFS values averaged over September 2002–August 2015 period. Red/blue indicate relatively high/low DOFS, respectively.

The global tropospheric ammonia distribution from AIRS

J. X. Warner et al.

Title Page

Abstract

Introduction

Conclusions

References

Tables

Figures

◀

▶

◀

▶

Back

Close

Full Screen / Esc

Printer-friendly Version

Interactive Discussion

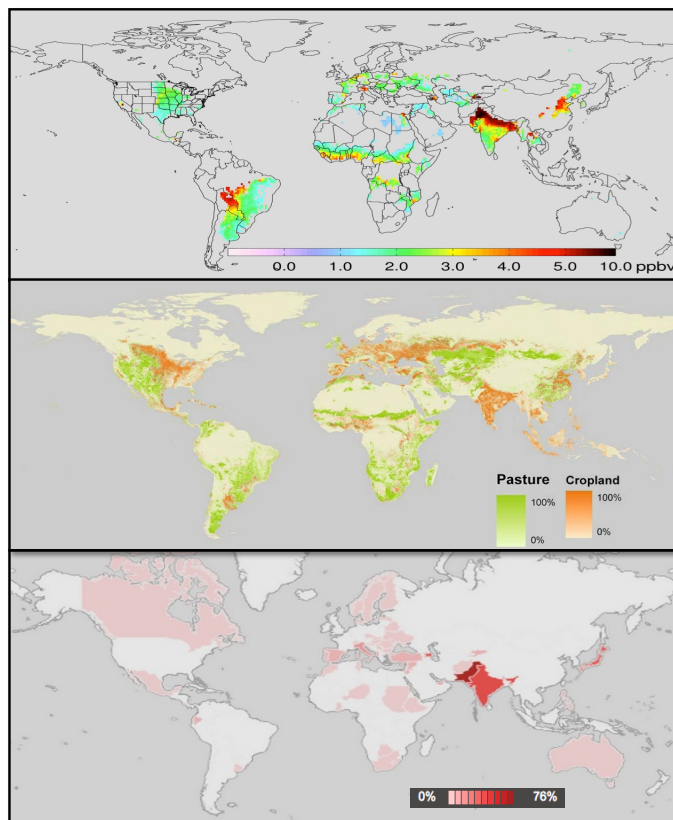


Figure 6. Top panel: the NH₃ VMRs from the persistent sources filtered with the collocated occurrences of elevated emissions (≥ 1.4 ppbv) using a threshold of 40 days; middle panel: pasture and cropland map (<http://OurWorldInData.org>); and bottom panel: irrigated agricultural land areas (data.worldbank.org).

The global tropospheric ammonia distribution from AIRS

J. X. Warner et al.

Title Page

Abstract

Introduction

Conclusions

References

Tables

Figures



Back

Close

Full Screen / Esc

Printer-friendly Version

Interactive Discussion

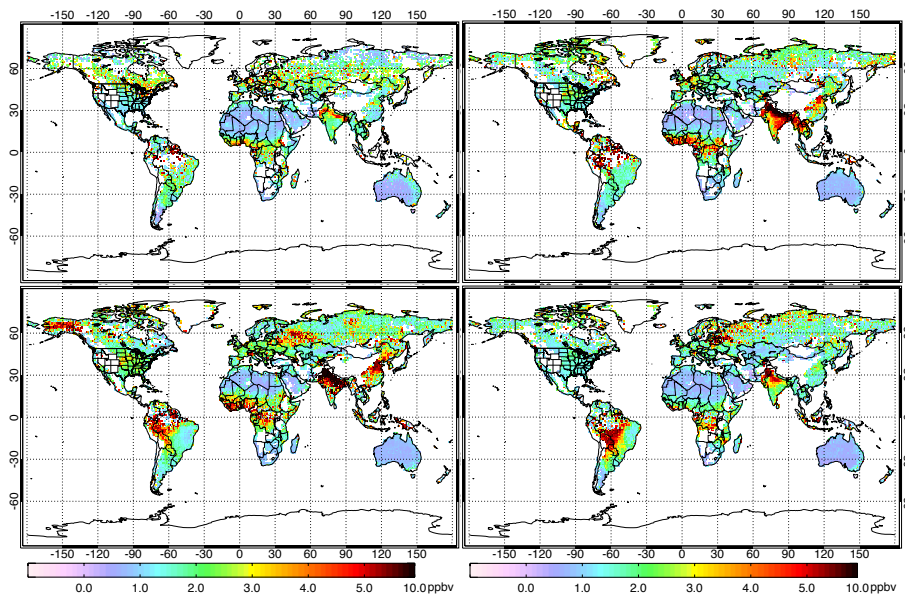


Figure 7. AIRS NH₃ VMRs at 918 hPa averaged between September 2002 and August 2015 for December–January–February (DJF, upper left panel), March–April–May (MAM, upper right panel), June–July–August (JJA, lower left panel), and September–October–November (SON, lower right panel), with DOFS greater than 0.1 and no cutoff limit for the VMRs. Red/purple indicate relatively high/low NH₃ VMRs.

The global tropospheric ammonia distribution from AIRS

J. X. Warner et al.

Title Page

Abstract

Introduction

Conclusions

References

Tables

Figures



Back

Close

Full Screen / Esc

Printer-friendly Version

Interactive Discussion

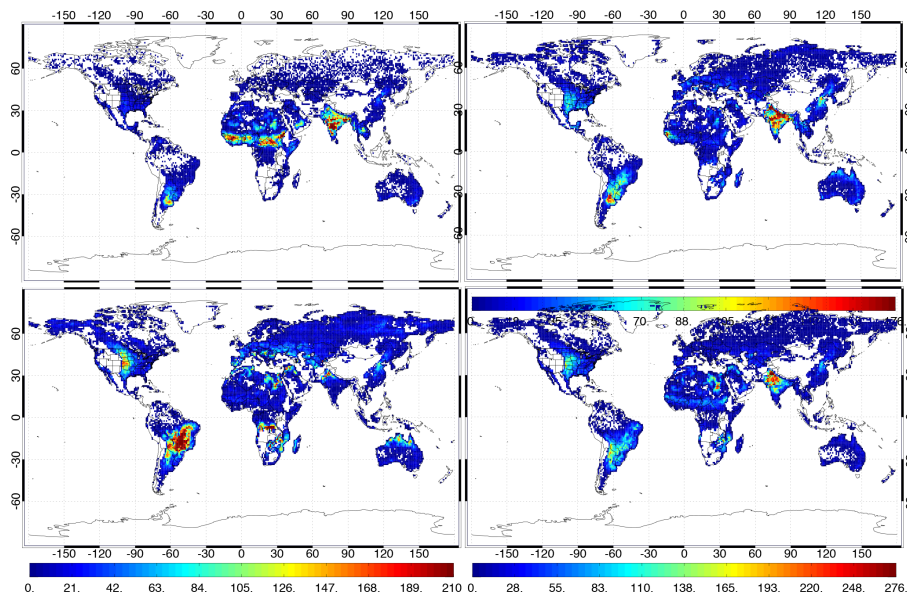


Figure 8. As in Fig. 7 except for the occurrences of high emissions ($\text{VMRs} \geq 1$ ppbv). Red/blue indicate relatively high/low occurrences of high emissions.

The global tropospheric ammonia distribution from AIRS

J. X. Warner et al.

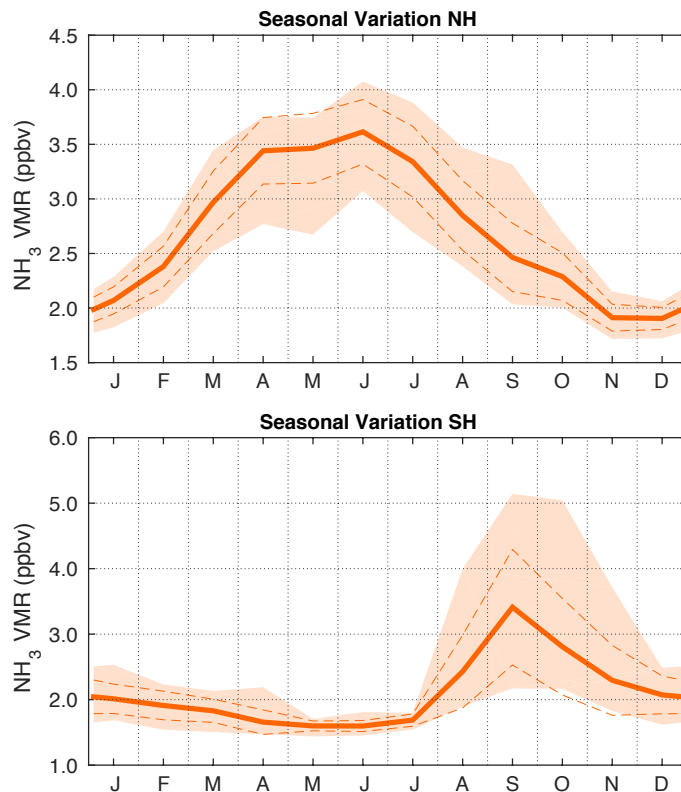


Figure 9. The NH₃ monthly mean variations (solid line) in the NH (upper panel) and the SH (lower panel), respectively. The long-dash lines show the 1σ standard deviation (SD); and the shaded areas represent the maximum and minimum range of each dataset.